Metamaterial-based perfect absorber: polarization insensitivity and broadband

OPEN ACCESS

IOP Publishing | Vietnam Academy of Science and Technology

Advances in Natural Sciences: Nanoscience and Nanotechnology

Adv. Nat. Sci.: Nanosci. Nanotechnol. **5** (2014) 025013 (7pp)

doi:10.1088/2043-6262/5/2/025013

Metamaterial-based perfect absorber: polarization insensitivity and broadband

Thi Hien Nguyen[1], Son Tung Bui[1], Trong Tuan Nguyen[1], Thanh Tung Nguyen[2], YoungPak Lee[3], Manh An Nguyen[4] and Dinh Lam Vu[1]

[1] Institute of Materials Science, Vietnam Academy of Science and Technology, 18 Hoang Quoc Viet, Hanoi, Vietnam

[2] Laboratory of Solid State Physics and Magnetism, Department of Physics and Astronomy, Katholieke Universiteit Leuven, 3001 Leuven, Belgium

[3] Quantum Photonic Science Research Center and Department of Physics, Hanyang University, Seoul 133–791, Korea

[4] Hong Duc University, 307 Le Lai, Đong Son, Thanh Hoa, Vietnam

E-mail: lamvd@ims.vast.ac.vn

Received 9 April 2014
Accepted for publication 14 April 2014
Published 7 May 2014

Abstract

We report the design and simulation of a microwave metamaterials-based perfect absorber using a simple and highly symmetric structure. The basic structure consists of three functional layers: the middle is a dielectric, the back is a metallic plane and the front is a ring of metal. The influence of structural parameters on the absorbance and absorption frequency were investigated. The results show an exceptional absorption performance of near unity around 16 GHz. In addition, the absorption is insensitive to the polarization of the incident beam due to the highly symmetric structure. Finally, four and nine rings with different sizes are arranged appropriately in a unit cell in order to construct a broadband absorber. A polarization-insensitive absorbance of above 90% is achieved over a bandwidth of 15%.

Keywords: metamaterials, perfect metamaterial absorber, broadband metamaterial absorber
Classification numbers: 5.17

1. Introduction

Over the past decade, a new class of artificial materials, the so-called metamaterials (MMs), has shown many unusual properties, which are not found in natural materials, such as materials with simultaneously negative permittivity and permeability leading to negative refractive index [1–3] and numerous fascinating applications such as perfect lens [4] and invisible cloaking [5, 6]. Recently, the applicability of MMs as electromagnetic wave absorbers has been attracting the interest of many scientists from the viewpoint of feasible MM applications using current technology. A near unity absorber is a device in which all incident radiation is absorbed at the operating frequency. The transmission, reflection and all other light propagation channels are disabled [7]. Electromagnetic wave absorbers can be used in devices and areas such as: emitters [8–10], sensors [11], spatial light modulators [12], IR camouflage [7, 13], thermophotovoltaics and wireless communication [14]. In 2008, Landy *et al* proposed a thin metamaterial absorber (MA), in which electric and magnetic responses are manipulated to make the impedance of absorber match to that of air and the imaginary part of the refractive index acquire a very large value simultaneously [15]. Therefore, the reflection and transmission are eliminated and the incident wave is strongly absorbed. Initial interest in electromagnetic wave absorbers was largely in the microwave range. The usefulness of absorbers in both improving radar performance and providing concealment against radar systems was utilized as a military technique. Since the first proposal of Landy, many groups have successfully designed and manufactured perfect MA from the microwave to the optical region [16–22]. In earlier works, because the strong absorption just occurs at the resonant frequency, the absorption bandwidth is often narrow. In many cases, broadband absorption is required, such as solar energy harvesting [23]. Up to now, many such absorbers have been computationally

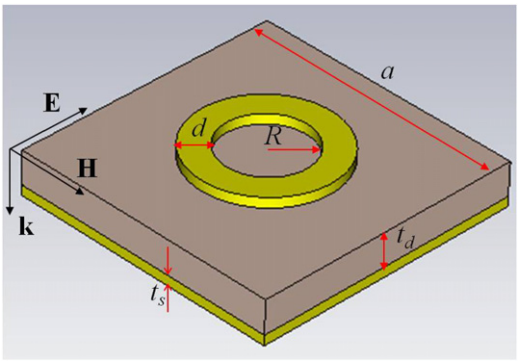

Figure 1. A schematic drawing of a unit cell of ring structure, polarization, and geometrical parameters.

and experimentally demonstrated and various techniques have been used to realize multiple band and broadband absorbers. The first method utilizes multiple resonating structures in each unit cell, exploiting the resonators with different sizes resonating at different frequencies. By combining them in one unit cell, multiple resonances will appear in the absorption spectrum. If these absorption resonances are close enough in frequency, they will form a broadband absorption. Another method is stacking multiple layers in which resonators share the same ground plane, but the fabrication is not really easy [24]. Another method utilizes the different sections of a single structure that resonate at different frequencies to obtain multiple resonances [25]. However, the existing obstacle is the polarization sensitivity. Recently, another approach to realize broadband absorption, that is incorporating lumped elements into the MM resonators, seems to have been a promising way for microwave frequencies [26]. Although adding lumped elements is an interesting idea, the feasibility in high frequency ranges such as near IR or optical region is still a problem due to the small size of MM resonator [7]. In this study, we propose and simulate an absorbing structure in the microwave region with simple and highly symmetric geometry. The influence of structural parameters and electromagnetic polarization on the absorption is investigated and the loss mechanism is also discussed. Then, a broadband absorber is constructed using the proposed structure. Finally, the dependence of broadband absorption on polarization is studied to assess the absorption efficiency.

2. Design and simulation

Numerical simulations of the design are performed by using a finite-integration-technique package of CST Microwave Studio. A unit cell of proposed MA is made of a dielectric layer sandwiched between a copper ring and a copper film, as shown in figure 1. The dielectric layer is lossy flame retardant 4 (FR-4) with the thickness of $t_d = 0.4$ mm, a determined dielectric constant of 4.0 and a loss-tangent of 0.025. The thickness of the copper strips in FR-4 board is $t_s = 0.036$ mm with an electric conductivity of 5.96×10^7 S m^{-1}. The geometrical parameters are set to be $a = 8$ mm, $d = 0.8$ mm, $R = 1.3$ mm. The direction of incident wave **k** is parallel to the axis of the ring while **E-H** plane is normal. The boundary conditions are set so that the unit cells are periodic in the **E-H** plane. The environment of simulation is performed in free space. We use TEM plane wave to stimulate the single unit cell, which provides S parameters in order to calculate the absorbance. The absorption power $A(\omega)$ is calculated through $A(\omega) = 1 - R(\omega) - T(\omega) = 1 - |S_{11}|^2 - |S_{21}|^2$, where the reflection power $R(\omega) = |S_{11}|^2$, and the transmission power, $T(\omega) = |S_{21}|^2$.

3. Resutls and discussion

3.1. Perfect metamaterial absorber based on ring structure

So far, a number of perfect absorption structures have been found, but with restrictions due to their complex structure and the difficult fabrication, especially in the optical region [27, 28] or polarization dependence [15]. To overcome the above disadvantages, we designed a simple structure with high symmetry, the so-called ring structure. In the current work, we systematically investigated the electromagnetic characterizations and the geometrical dependence of a perfect absorber based on this structure. The absorbance is calculated by $A(\omega) = 1 - R(\omega) - T(\omega) = 1 - |S_{11}|^2 - |S_{21}|^2$, as aforementioned. From the theoretical point of view, unity absorbance can be possibly achieved at certain frequency by reducing reflection and transmission to zero simultaneously. The minimum reflection can be obtained by matching the impedance of the sample to the air at resonance frequency. However, the transmission is zero, since the copper film acts as a physical barrier to block the incident waves. Figure 2(a) shows simulated results of reflectance, transmittance and absorbance of MA using ring structure. The perfect absorbance is observed at 16 GHz with no transmission and no reflection. One half of the ring in the direction of the electric field can be regarded as an electric dipole yielding an electric resonance, while the front ring and back metal film behave like the cut-wire pair structure responding for a magnetic resonance [29]. By changing the geometrical parameters of the ring, the electric and magnetic responses of MA can be controlled. Finally, the impedance matching condition is achieved at 16 GHz leading to perfect absorbance at this frequency. The influence of electromagnetic polarization on the absorption is examined in figue 2(b). It is shown that the polarization of the normal incident wave does not affect the absorption spectrum. The result can be explained due to the symmetry of the absorber in the **E-H** plane. Figure 2(c) is the simulation surface currents at absorption frequency. The opposite direction currents are generated on surfaces of the ring and the copper film while **H** field is polarized parallel to copper ring and film. Therefore, the anti-parallel currents are magnetic response and indicate that a magnetic resonance is formed at absorption frequency [29].

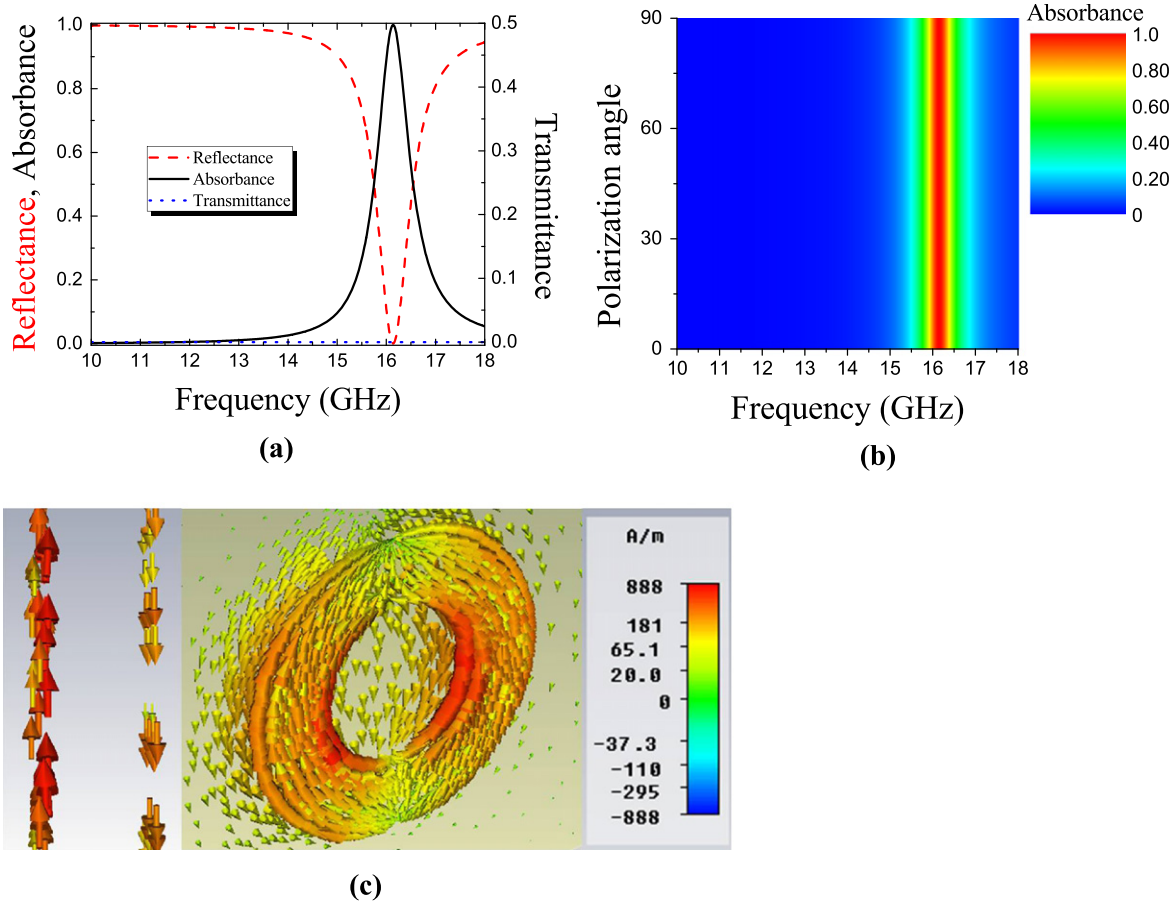

Figure 2. (a) Simulated results of reflectance, transmittance and absorbance. (b) Absorption spectra according to the polarization angle of the incident wave. (c) Distribution of induced current at the absorption frequency. From the left to the right: view in **E-k** plane, view in 3-dimension space, and scale of intensity.

One primary concern of MAs is what is mainly responsible for the losses. As mentioned above, the resonance is magnetic response verified by anti-parallel currents on surfaces of ring and metal film. Such resonance confines electromagnetic energy in unit cells and it is gradually eroded by two mechanisms of losses—those are dielectric and conductive. In order to get definite conclusions about the mechanism of energy dissipation in the proposed structure, we simulated power loss densities at ring, metallic film, and dielectric spacer as shown in figure 3. The loss is principally dissipated in the dielectric spacer, but the loss is not equally distributed in the spacer. It locates mainly at the edges of ring, where the effective capacitances are formed. The results definitely imply that the dielectric loss plays the key role in the energy dissipation mechanism. Our results are consistent with previous researches [8, 30].

3.2. Influence of structural parameters

The magnetic resonance frequency is usually strongly dependent on structural parameters [29]. As shown in figure 2(c), the magnetic resonance is formed at absorption frequency of the MA. For these reasons, we also investigated the influence of structural parameters on the absorption properties.

In figure 4(a), there is a pronounced shift towards the lower frequency of the absorption peak when the radius of the ring R increases. In the case of the width of the ring d in figure 4(b), the absorption peak shows the red-shift behavior too, but the shift is less than that in the previous case with the ring R. The influence of geometry parameters R and d on the absorption frequency is explained by the model of Zhou *et al* [29]. In ring structure, parameters R and d play a similar role to the length of cut-wire [31]. The manipulation of R and d changes the position of magnetic resonance that shifts the absorption frequency. In contrast, the absorption frequency is almost constant when the lattice constant a is larger than 7 mm and only changes with the smaller lattice constant, as shown in figure 4(c). The interpretation is that when the lattice constant is small, rings of adjacent unit cell are close to each other. Therefore, the interactions between the adjacent rings occur and shift the resonance frequency. When lattice constant is larger than a certain value, the interaction can be considered as negligible. The resonance position depends only on parameters of the ring in the unit cell and does not depend on lattice constant. In figures 4(a)–(c) we also investigated the dependence of absorbance on the parameters R, d, a. The results show that absorbance is maximized at certain values of R, d, a (approximately 100%). It is explained

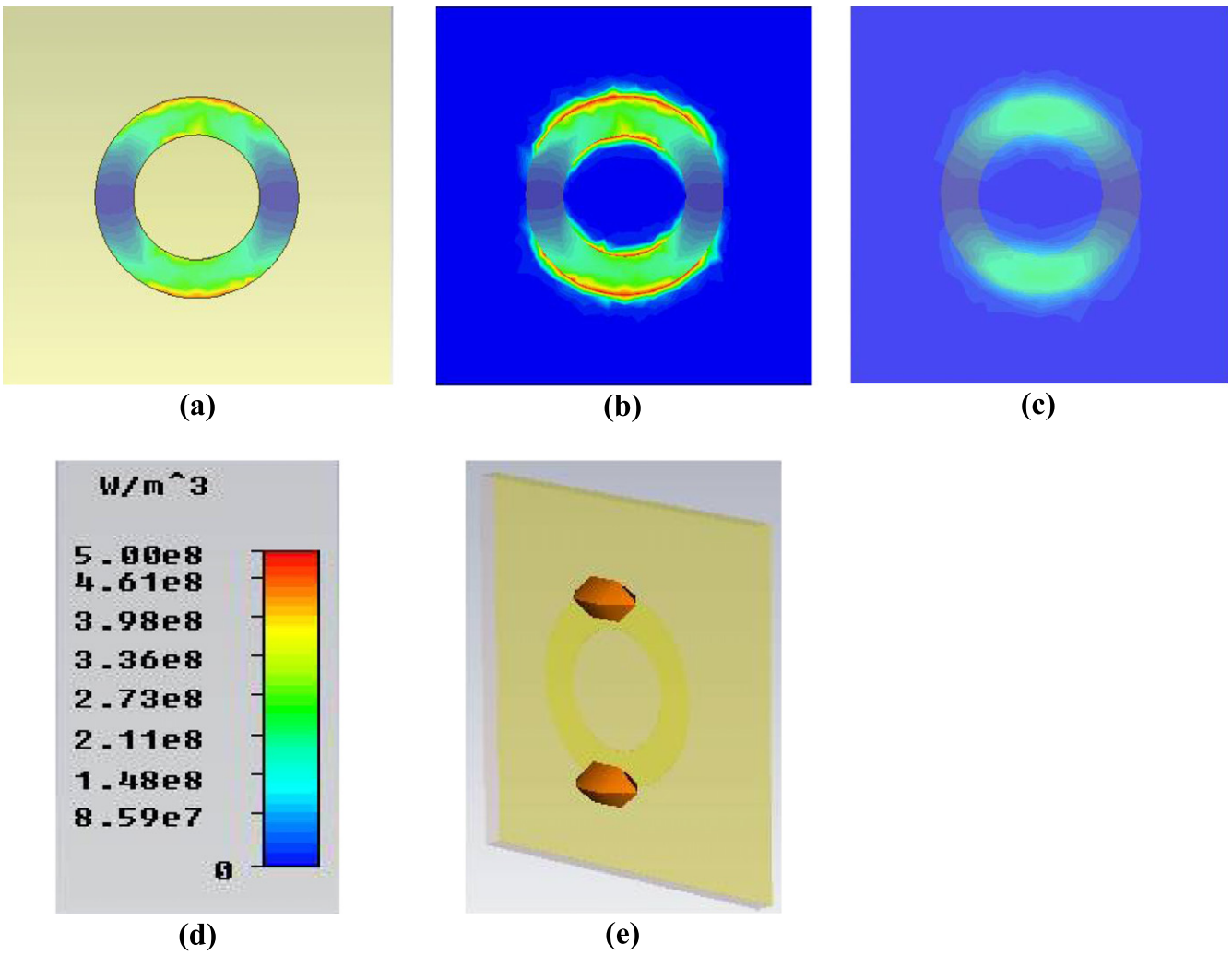

Figure 3. Simulated power loss densities in (a) copper ring, (b) dielectric substrate, (c) copper film at absorption frequency in the **E-H** cutting plane, and (d) scale of intensity. (e) Distribution of power losses at absorption frequency in the 3-dimension space.

that the impedance matching condition just occurs with certain geometry parameters, where the real part of impedance $\mathrm{Re}\,(z_{eff}) = \mathrm{Re}\left(\mu_{eff}/\varepsilon_{eff}\right) = 1$. Any fluctuation from these parameters changes value of either ε_{eff} or μ_{eff}. Consequently, the reflection raises up that decreases the absorbance. Nevertheless, the interesting result is that the absorbance is contrary to the absorption frequency when changing the MA parameters. With a small change of parameter R or d (change step is 0.1 mm), the absorbance is nearly unchanged while the absorption frequency is clearly shifted. The same contrary also exists in the case of changing the lattice constant a with the roles switched. With a quite large change of a (change step is 1 mm), the absorbance is significantly changed while the absorption frequency is almost invariable. The achieved results in this section suggest that the absorbance and absorption frequency can be controlled independently by adjusting different structural parameters. The above conclusion has a great significance with respect to the creation of the broadband absorber.

3.3. Broadband metamaterial absorber

In order to create a broadband absorber, we arranged the ring with different sizes at the front side of one unit cell, as shown in figure 5.

The four-peaks spectrum of absorbance with $R_1 = 1.3$ mm, $R_2 = 1.4$ mm, $R_3 = 1.5$ mm, $R_4 = 1.6$ mm and lattice constant $a = 14$ mm, $d = 1$ mm, is shown in figure 6(a). The result shows that peaks at 12.91, 13.42, 14.13, 14.93 GHz are individually excited by different rings. The magnetic field distributions at these frequencies are shown in figure 6(b) to better understand the physics of the proposed multi-band absorption of the MA. It is obvious that, at a certain frequency, the magnetic field is localized and absorbed at some ring in the unit cell. At higher frequency, the magnetic field is localized at the ring with less radius and vice versa. Therefore, in order to obtain the broadband absorption, we added rings with different radii in the unit cell and these radii are very close to each other. Figure 6(c) plots the broadband absorption spectrum for the model 9-rings MA: $R_1 = 1.50$ mm, $R_2 = 1.58$ mm, $R_3 = 1.66$ mm, $R_4 = 1.74$ mm, $R_5 = 1.82$ mm, $R_6 = 1.90$ mm, $R_7 = 1.98$ mm,

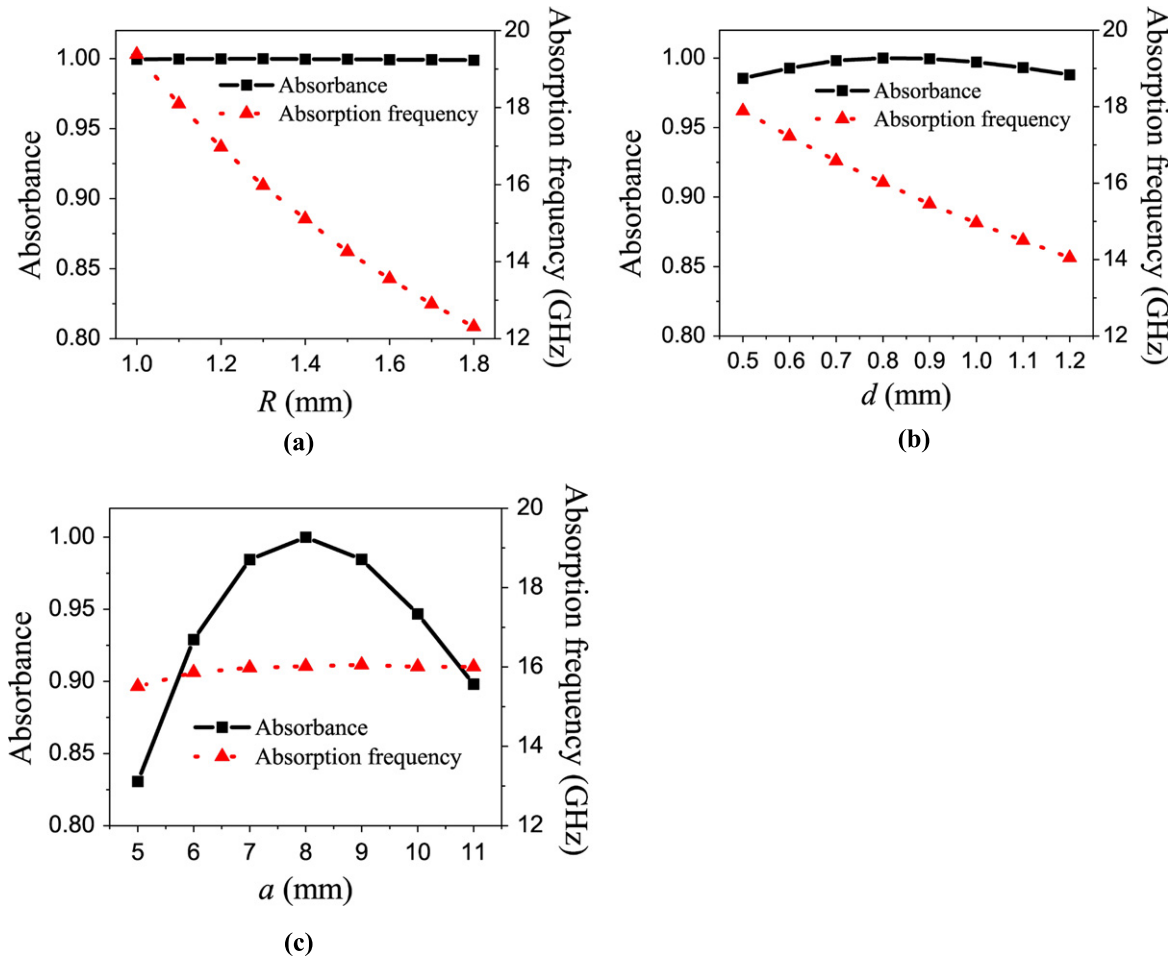

Figure 4. Dependence of the absorbance and absorption frequency on the MA parameters: (a) radius of ring R, (b) width of ring d and (c) lattice constant a.

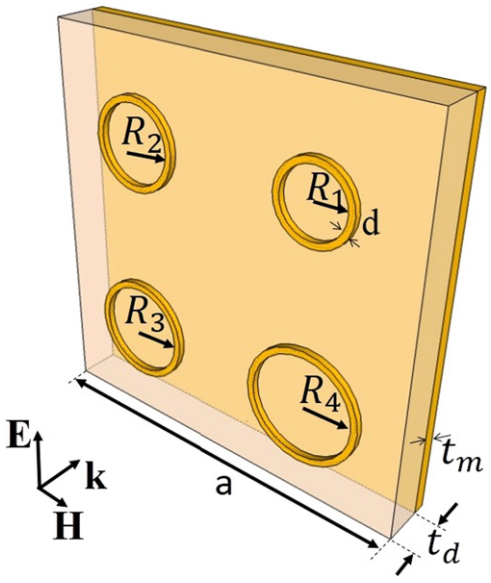

Figure 5. The unit cell of metamaterial structure consiting of 4 rings with different size.

$R_8 = 2.06$ mm, and $R_9 = 2.14$ mm, $a = 30$ mm, $d = 1$ mm. The result shows that an absorbance better than 90% is achieved within a bandwidth of over 2 GHz. The maximum of absorbance is nearly 100% from 12.2 to 12.5 GHz. Moreover, owing to the symmetric geometry of ring, broadband absorption exhibits nearly polarization-insensitive property under the normal incidence. Figure 6(d) shows absorption spectra according to the polarization angle ϕ. The broadband absorption is not changed so much when enhancing ϕ from 0° to 60°.

4. Conclusions

We studied numerically and experimentally the electromagnetic properties of perfect microwave MAs using ring and multi-ring structures. It is shown that by inducing a magnetic resonance, the ring structure confines electromagnetic energy at the resonant frequency. This energy mainly dissipates in the dielectric spacer, causing a near unity absorbance. Our investigation implies that the absorption frequency, strength, and bandwidth of ring-based MAs can be tailored nearly at will by systematically controlling geometrical parameters. Based on these findings, the broadband MA was designed,

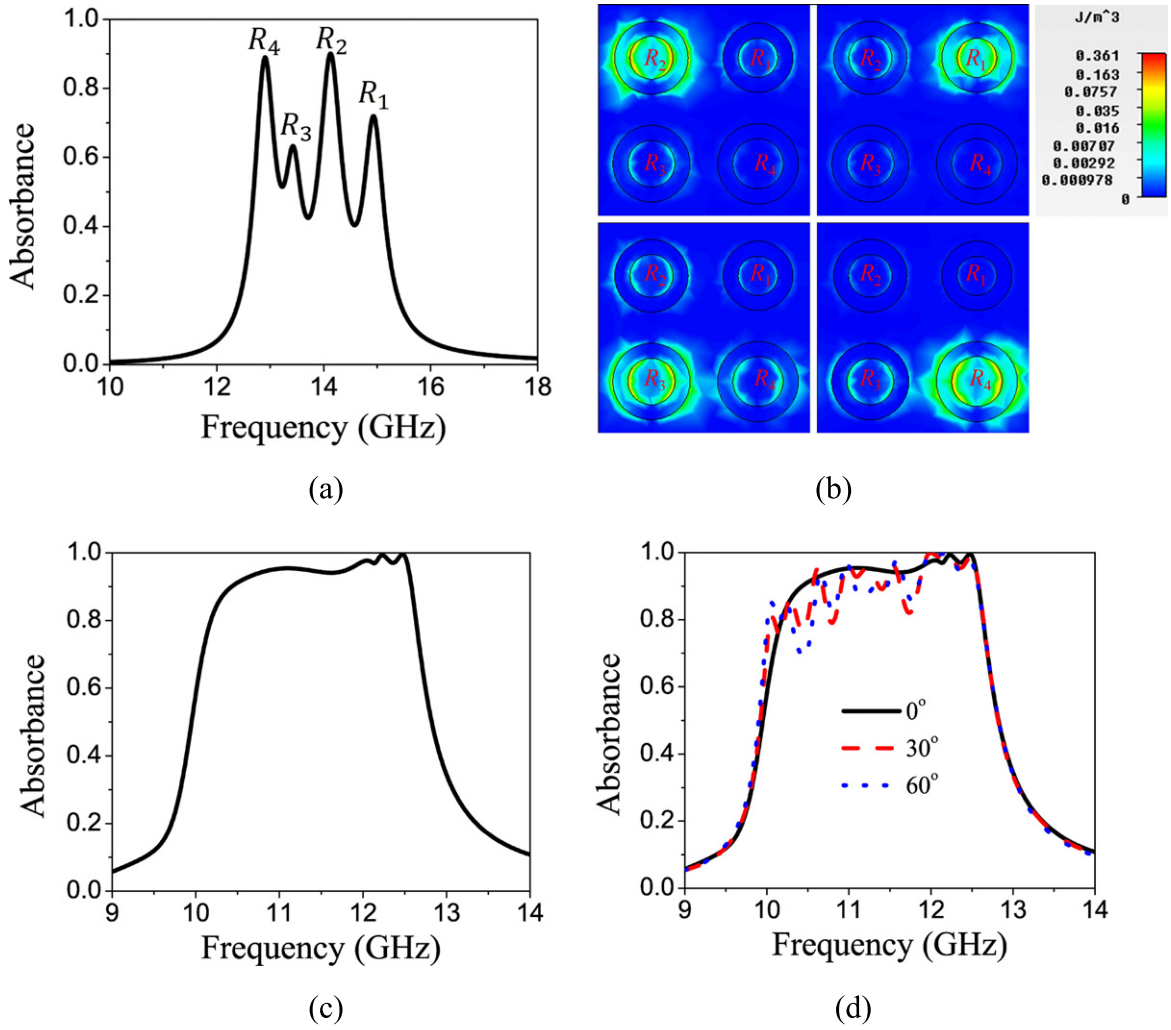

Figure 6. (a) Absorption spectrum of 4-rings absorber. (b) Simulated induced magnetic distributions at absorption frequencies and scale of intensity: the anti-clockwise direction is corresponding to the decrease of absorption frequency; the top right figure is the simulation at 14.93 GHz. (c) Absorption spectrum of broadband absorber of 9-rings. (d) Absorption spectra of broadband absorber according to polarization angle of the incident wave.

simulated, and measured, showing an excellent absorbance, broad absorption bandwidth, and polarization insensitivity.

Acknowledgments

This work in Vietnam was supported by the National Foundation for Science and Technology under grant no. 103.02-2013.54.

References

[1] Veselago V G 1968 *Sov. Phys. Usp.* **10** 509514
[2] Smith D R, Padilla W J, Vier D C, Nermat-Nasser S C and Schultz S 2000 *Phys. Rev. Lett.* **84** 4184
[3] Shelby R A, Smith D R and Schultz S 2001 *Science* **292** 77
[4] Pendry J B 2000 *Phys. Rev. Lett.* **85** 3966
[5] Pendry J B, Schurig D and Smith D R 2006 *Science* **312** 1780
[6] Schurig D, Mock J J, Justice B J, Cummer S A, Pendry J B, Starr A F and Smith D R 2006 *Science* **314** 977
[7] Watts C M, Liu X and Padilla W J 2012 *Adv. Mater.* **24** OP98–120
[8] Liu X, Tyler T, Starr T, Starr A, Jokerst N M and Padilla W J 2011 *Phys. Rev. Lett.* **107** 045901
[9] Chang Y C, Wang C M, Abbas M N, Shih M H and Tsai D P 2009 *Opt. Express* **17** 13526
[10] Lai J J, Liang H F, Peng Z L, Yi X and Zhai X F 2011 *J. Phys.: Conf. Ser.* **276** 012129
[11] Liu N, Mesch M, Weiss T, Hentschel M and Giessen H 2010 *Nano Lett.* **10** 2342
[12] Chan W L, Chen H T, Taylor A J, Brenner I, Cich M J and Mittleman D M 2009 *Appl. Phys. Lett.* **94** 213511
[13] Bienz E F 1979 *US Patent* 4142015
[14] Singh P, Korolev K A, Afsar M N and Sonkusale S 2011 *Appl. Phys. Lett.* **99** 264101
[15] Landy N I, Sajuyigbe S, Mock J J, Smith D R and Padilla W J 2008 *Phys. Rev. Lett.* **100** 207402
[16] Landy N I, Bingham C M, Tyler T, Jokerst N, Smith D R and Padilla W J 2009 *Phys. Rev.* B **79** 125104
[17] Tuong P V, Lam V D, Park J W and Lee Y P 2013 *Adv. Nat. Sci.: Nanosci. Nanotechnol.* **4** 035009
[18] Tuong P V, Park J W, Lam V D, Zheng H Y, Rhee J Y, Kim K W and Lee Y P 2013 *Adv. Nat. Sci.: Nanosci. Nanotechnol.* **4** 015001

[19] Liu X, Starr T, Starr A F and Padilla W J 2010 *Phys. Rev. Lett.* **104** 207403
[20] Liu N, Mesch M, Weiss T, Hentschel M and Giessen H 2010 *Nano Lett.* **10** 2342
[21] Lin C H, Chern R L and Lin H Y 2011 *Opt. Express* **19** 41
[22] Jiang Z H, Yun S, Toor F, Werner D H and Mayer T S 2011 *ACS Nano* **5** 4641
[23] Ding F, Cui Y, Ge X, Jin Y and He S 2012 *Appl. Phys. Lett.* **100** 103506
[24] Ye Y Q, Jin Y and He S 2010 *J. Opt. Soc. Am.* **27** 498
[25] Tao H, Bingham C M, Pilon D, Fan K, Strikwerda A C, Shrekenhamer D, Padilla W J, Zhang X and Averitt R D 2010 *J. Phys.* D **43** 225102
[26] Cheng Y Z, Wang Y, Nie Y, Gong R Z, Xiong X and Wang X 2012 *J. Appl. Phys.* **111** 044902
[27] Tao H, Bingham C M, Strikwerda A C, Pilon D, Shrekenhamer D, Landy N I, Fan K, Zhang X, Padilla W J and Averitt R D 2008 *Phys. Rev.* B **78** 241103
[28] Grant J, Ma Y, Saha S, Khalid A and Cumming D R 2011 *Opt. Lett.* **36** 3476
[29] Zhou J, Economon E N, Koschny T and Soukoulis C M 2006 *Opt. Lett.* **31** 36203622
[30] Viet D T, Tung B S, Quynh L V, Hien N T, Tuan N T, Tung T T, Lee Y P and Lam V D 2012 *Adv. Nat. Sci.: Nanosci. Nanotechnol.* **3** 045014
[31] Park J W, Jin X R, Tuong P V, Rhee J Y, Kim K W, Kim D and Lee Y P 2012 *Phys. Status Solidi* B **249** 858